International Journal of Applied Power Engineering (IJAPE)
Vol. 15, No. 2, June 2026, pp. 674~691
ISSN: 2252-8792, DOI: 10.11591/ijape.v15.i2.pp674-691

Performance evaluation of several basic types of DC-DC converters for small-scale wind turbine connected to isolated load

Rizki Mendung Ariefianto[1,2], Rini Nur Hasanah[1], Hadi Suyono[1], Tri Nurwati[1], Eduard Muljadi[3], Hazlie Mokhlis[2]
[1]Department of Electrical Engineering, Faculty of Engineering, Universitas Brawijaya, Malang, Indonesia
[2]Department of Electrical Engineering, Faculty of Engineering, Universiti Malaya, Kuala Lumpur, Malaysia
[3]Department of Electrical and Computer Engineering, College of Engineering, Auburn University, Auburn, USA

Article Info

Article history:

Received Oct 4, 2024
Revised Feb 13, 2026
Accepted Mar 12, 2026

Keywords:

Basic DC-DC converter
MPPT
Power extraction
SSWT
Wind energy

ABSTRACT

Small-scale wind turbines (SSWT) encounter a primary issue in power extraction, making the integration of DC-DC converters with maximum power point tracking (MPPT) crucial for performance enhancement. This study focuses on an evaluation of basic DC-DC converters, which offer many benefits when applied to SSWT systems. By considering efficiency, suitability, and electrical stress aspects, six DC-DC converter topologies consisting of boost, buck-boost, SEPIC, Cuk, zeta, and Luo, were tested under perturb and observe (P&O) and incremental conductance (INC) MPPT strategies. A 6.5-kW SSWT system, including a DC-DC converter and MPPT was designed in detail using PSIM. The results show that boost converter demonstrated the best overall performance in terms of power extraction, efficiency, and stress reduction, although its operation was limited to a narrower wind speed range. The zeta converter achieved efficiency and power extraction comparable to the boost converter with stable operation over a broader wind speed range, while the buck–boost converter offered step-up/step-down capability but experienced higher voltage and current stress. The SEPIC and Cuk converters showed low overall performance compared to others, whereas the Luo converter was better suited for low-wind-speed conditions.

Corresponding Author:

Rini Nur Hasanah
Department of Electrical Engineering, Faculty of Engineering, Universitas Brawijaya
St. MT Haryono 157, Lowokwaru, Malang 65145, Indonesia
Email: rini.hasanah@ub.ac.id

1. INTRODUCTION

As an archipelagic country, Indonesia has abundant resources of renewable energy resources, one of which is wind energy. This energy ranks second among the most abundant sources, with a technical potential of 60.6 GW [1]. Globally, wind energy is a favorable option since it requires minimal space, environmentally friendly, good maturity, and fast growing demand [2]-[4]. However, this potential is not well-reflected in actual implementation. Until 2023, the installed capacity of wind turbines in Indonesia had reached only 0.25% of its technical possible extraction [5]. One of the main obstacles is the existence of widely dispersed islands, which makes it difficult to develop an efficient and beneficial configuration due to high investment costs and incurs inefficient maintenance. Hence, wind energy emerges as one of the solutions in these regions. In standalone systems, wind energy extraction can be achieved by installing small-capacity wind turbines. Indonesia has

wind speeds ranging from 2 to 6 m/s, corresponding to turbine capacities of approximately 0.5 to 10 kW. It is obvious that a small-scale wind turbine (SSWT) is highly suitable for island territory. For instance, this SSWT can be installed on rooftops or dedicated land areas.

Unfortunately, attaining optimal energy transfer in wind systems poses a significant challenge, primarily due to fluctuations in wind speed [6]. Hence, employing a DC-DC converter addresses that issue and ensures the continuous operation of wind turbines [7]. In most applications, DC-DC converters not only increase the voltage level but also preserve power generation near the maximum extractable level by referring the peak point of turbine's power curve. These converters typically regulate the power output of small wind turbines using maximum power point tracking (MPPT) techniques [8], [9]. Various DC-DC converter architectures have been developed to achieve higher efficiency, implement reliable switching strategies, incorporate fault-tolerant features, and cater specifically to renewable energy applications [10]. Therefore, the main considerations in selecting an appropriate DC-DC converter for wind energy applications relate to two key factors: the intrinsic efficiency of the converter and its performance in enhancing MPPT effectiveness. The former is particularly influenced by the converter's topology, which is associated with the number of electrical components used, and the latter emphasizes the DC-DC converter must ensure high-efficiency power extraction while minimizing power losses.

Before assessing the performance enhancement of DC-DC converters through configuration design, it is essential to recognize the basic converter types to obtain better advantages. This is attributed not only to their simplicity and low cost but also to their well-established performance in real-world applications. Basic converters typically utilize a single-switch concept, making them more practical compared to modified types that incorporate multiple switches. These devices are classified as part of power electronic converters and represent a substantial portion of the overall cost of wind turbine applications. Several basic DC-DC converter topologies, such as boost, buck, and buck-boost converters, are commonly applied individually in wind turbine systems. In SSWT applications, step-up DC-DC converters are generally favored due to the necessity for voltage conversion to higher levels to enable grid interconnection [11]. However, when the turbine output voltage is lower than the battery voltage, conversion becomes infeasible, highlighting the limitations of boost-only converters. Conversely, the buck-boost converter is sometimes preferred, as it offers greater flexibility in both increasing and decreasing input voltage [12]. To evaluate and compare the performance of both converter types, further analysis is required to determine their practical suitability. It is important to note that these converters belong to the basic DC-DC converter family. Although numerous converter variations may demonstrate optimal performance in simulations or lab-scale experiments, many of them remain unadopted in commercial or utility-scale systems. Therefore, it is crucial to conduct a comprehensive evaluation of basic DC-DC converters and to define broader classification boundaries for them, thereby providing more informed options for selecting converters in SSWT applications.

Many researchers have proposed various basic DC-DC converter architectures for SSWT, particularly for standalone applications. A 500 W-SSWT based on a boost converter was proposed. The application of this converter yielded a remarkable MPPT efficiency of 93.87% [13]. Building upon this, the results in [14] introduced linear matrix inequalities (LMI) control applied to a SEPIC converter for wind turbines. The integration of LMI control not only maintained high efficiency in energy conversion but also introduced a refined control strategy for optimizing the power extraction process. The synergy of converter technologies and control strategies emerged as a key focus in advancing wind turbine technologies. An MPPT method based on modified perturb and observe (P&O) for a 3-kW wind turbine with a permanent magnet synchronous generator (PMSG) and boost converter was evaluated [15]. Through rigorous testing under varying conditions, the modified MPPT system demonstrated a 50.77% increase in average power output, representing a significant enhancement in MPPT adaptation. A similar work in [16] also employed a boost converter with advanced MPPT algorithms. Further research by [17] explored a Zeta converter combined with a multi-mode control strategy for wind turbine battery management, illustrating its potential for improved energy storage performance. A related concept of 3-kW SSWT-battery system using the P&O algorithm was presented in [18]. This research employed a buck-boost converter as an electrical interface, leading to empower operation on a broader scale of wind speed. An interleaved buck-boost converter was introduced by [19] for 19-kW SSWT, employing a P&O-based MPPT method. This converter gives the most optimal performance by achieving 96.8% efficiency. A voltage-lift boost converter driven by a hybrid MPPT strategy was implemented in 12-kW off-grid wind turbine system [20]. The converter exhibits higher performance, raises the voltage gain, improves efficiency, and is feasible for low-power wind turbines. A comparative study using buck-boost, Cuk, and SEPIC converters for a 24-kW SSWT was conducted in [21]. At a rated constant wind speed of 12 m/s, the SEPIC converter demonstrated the highest efficiency at 93.2%, making it the most suitable among the evaluated types. These cumulative advancements represent the state of the art in wind turbine technology, shaping the landscape for sustainable and efficient wind energy utilization in the foreseeable future.

Despite these efforts, many of the above studies lack comprehensive evaluation of DC-DC converters in the context of SSWT. Additionally, they often focus more on the MPPT algorithms rather than the critical

role of the converter topology. More broadly, research exploring the integration of DC-DC converters in SSWT applications remains limited. When discussing SSWT systems, most studies focus on mechanical aspects, such as aerodynamics, blade design, rotor configuration, and turbine materials. In terms of electrical systems, many studies are confined to comparative MPPT analyses, with the converter's influence typically demonstrated only at rated wind speed conditions. For DC-DC converter assessment, comparative studies often rely on assumed or fixed source profiles. Moreover, research dedicated to DC-DC converter applications in wind turbines is less prevalent than that for photovoltaic systems.

These limitations must be solved, as SSWT systems are critical for the development of decentralized renewable energy infrastructure. Therefore, the main contributions of this study are summarized as follows:

- Several basic DC-DC converter topologies are evaluated and compared to determine the most suitable configurations for SSWT systems. This is characterized by an investigation of their power extraction capabilities, as well as parameters such as voltage gain, semiconductor stress, efficiency, and power losses.
- This study proposes a selection framework for basic DC-DC converters, considering factors such as topological simplicity, non-isolated structure, buck-boost capability, and unidirectional power flow.
- The converter performance is assessed not only at rated wind speeds but also across a range of wind speed levels, emphasizing the ability to produce enormous power even at low wind speeds, thus illustrating the minimum cut-in speed of SSWT supported by the converter.
- The selected converters are also tested with two different MPPT methods to highlight the influence of converter topology on MPPT performance.

To accomplish these objectives, an SSWT system with identical ratings is modeled in PSIM software for all converter simulations. The detailed simulation processes, including block diagrams, are provided. The results aim to offer valuable insights into the effectiveness of basic DC-DC converters in SSWT applications and serve as a practical reference for selecting a suitable converter for various wind energy scenarios.

2. METHOD

Figure 1 shows a flowchart depicting the evaluation process of basic DC-DC converters suitable for SSWT systems. Overall, the evaluation is conducted in several stages. First, the design phase involves the development of a 6.5-kW SSWT model and the formulation of mathematical equations for power extraction within the simulation block. Second, the selection of basic DC-DC converters is carried out by considering several key factors, including topological simplicity, non-isolated structure, buck-boost capability, and unidirectional power flow. Once a converter that meets these criteria is identified, a design calculation process is conducted to determine the appropriate component values. Third, basic MPPT algorithms such as P&O and incremental conductance (INC) are applied for each converter to validate its performance under variable wind speed. Fourth, simulations are performed under various wind speed conditions, ranging from low to rated wind speeds. This stage also includes the evaluation of cut-in speed capability, which is influenced by the converter's performance. Finally, a comparative analysis is conducted by assessing several parameters, including extracted power, MPPT efficiency, SSWT efficiency, voltage gain, voltage stress, current stress, power losses, and the overall efficiency of each converter.

2.1. Small scale wind turbine design

In the initial stage, an SSWT with a rated power of 6.5 kW was designed. It is assumed that the turbine operates at the nominal wind speed (v_w) of 12 m/s. It is necessary to have a mathematical model that is capable of adequately simulating the stochastic dynamics present in the behavior of the wind, including both its constant behavior and its variations in the form of gusts, slopes, and disturbances. In this way, wind modeling is done by the sum of these four components, given in m/s, as shown in (1).

$$v_w(t) = v_b(t) + v_r(t) + v_g(t) + v_n(t) \quad (1)$$

Where v_b is the constant of the base component of the wind, v_r is the portion relating to ramp variations, v_g is the component related to bursts, and v_n is the component related to disturbances. However, as the focus of the present work is to study connection strategies for the wind turbine to the electrical power system, it is considered that the wind dynamics are represented only by the component in step $v_b(t)$.

The primary function of the wind turbine is to extract the kinetic energy present in the wind into rotational kinetic energy, making it a viable source of primary energy through the electromechanical energy conversion process. In a steady state condition, both the extracted power and the mechanical torque applied to the wind turbine shaft are represented by (2) and (3), respectively.

$$P_m = {}^1/_2\, C_P(\lambda,\beta)\, \rho\, \pi R^2\, v_w^3 \quad (2)$$

$$\tau_m = {}^1/_{2\lambda}\, C_P(\lambda,\beta)\, \rho\, \pi R^3\, v_w^2 \quad (3)$$

Where C_P is the power coefficient, ρ is the air density, β is the angle of attack of the blades in relation to the plane of wind displacement, v_w is the wind speed, and λ is the relationship between the tip speed of the propellers and the wind speed given in (4).

$$\lambda = \frac{\omega_r R}{v_w} \quad (4)$$

Where ω_r and R are the angular speed of the blades and the turbine's radius. In (5), the set of curves that define the coefficient C_P is presented, in which the parameter λ_i shown in (6) is a function that contains the tip speed ratio (λ) and the pitch angle of the turbine (β).

$$C_P(\lambda,\beta) = 0.5\left(\frac{116}{\lambda_i} - 0.4\beta - 5\right) e^{-\frac{21}{\lambda_i}} + 0.012\lambda \quad (5)$$

$$\lambda_i = \frac{1}{\frac{1}{\lambda+0.08\beta} - \frac{0.035}{\beta^3+1}} \quad (6)$$

From this scenario, it is obvious that the condition of maximum power extraction is defined by the choice of the parameter λ in such a way that the power coefficient C_P is the largest possible. To achieve the highest peak point of the wind turbine performance curve, the coefficient λ is varied in relation to the parameter C_P, considering that the angle of attack β is zero. The turbine curve used in this study can be constructed based on mathematical expressions to acquire the C_P value, as shown in Figure 2(a). Assuming the pitch angle (β) is set to zero, indicating the wind turbine efficiency is solely affected by tip speed ratio, this process obtains a nonlinear efficiency curve, as depicted in Figure 2(b). The peak value of the C_P curve is approximately 0.4916, with the optimum λ occurring at around 8.18. Subsequently, the key parameters of the overall SSWT are presented in Tables 1 and 2.

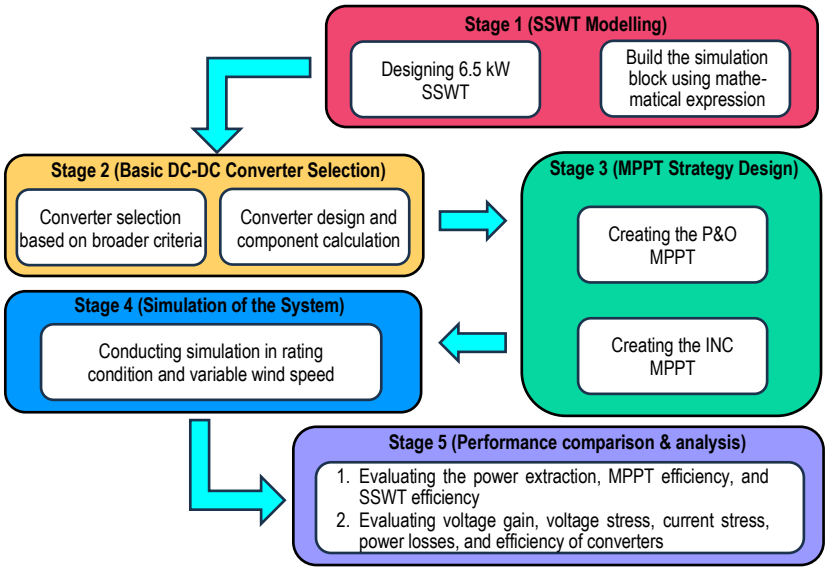

Figure 1. Framework of research method

Based on the simulation results, the C_P curve characteristics specify that the SSWT is capable of generating a rated power of 6.5 kW at a nominal wind speed of 12 m/s. At this point, the MPPT will reference the optimal power point, which applies to every wind speed as well. In Figure 3, the optimal power points of the SSWT are provided, ranging from 4 to 12 m/s wind speeds. It is important to note that the optimal power point is referenced to the electrical power point generated by the generator. This means that this electrical

power is slightly lower than the mechanical power of the turbine due to losses in the generator and rectifier. The embedded MPPT in the duty cycle generation of the DC-DC converter will utilize this reference of the optimal electrical power point from voltage and current sensing at the converter input.

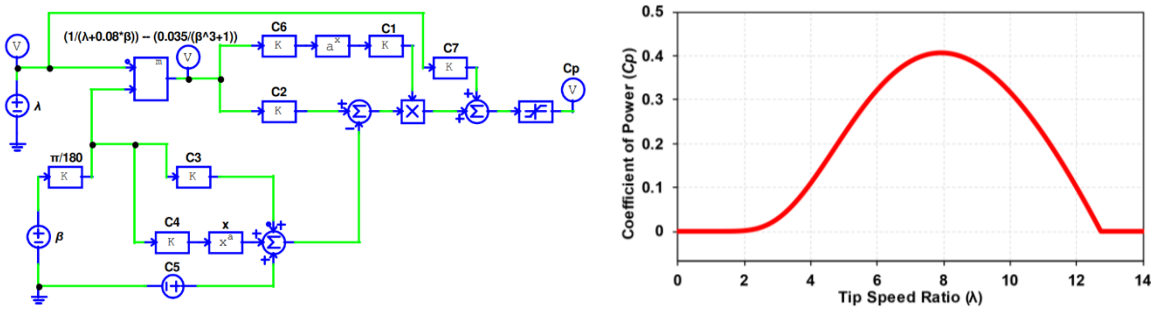

(a) (b)

Figure 2. C_P blocks of wind turbine in PSIM software: (a) mathematical expressions and (b) nonlinear efficiency curve

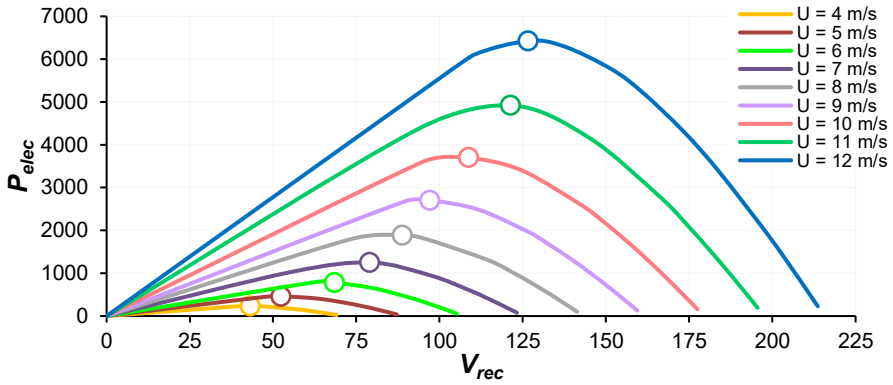

Figure 3. Maximum power point of 6.5-kW SSWT under various wind speed

Table 1. Wind turbine-generator specification

Turbine parameters	Specification
Turbine type	3-blade horizontal axis
Power rating (P_m)	6.5 kW
Nominal wind speed (U)	12 m/s
Turbine radius (R)	2 m
Nominal rotor speed (ω_r)	50 rad/s (470 rpm)
C_P maximum and λ optimum	0.4916 and 8.18

Table 2. Generator specification

Generator parameters	Specification
Generator type	PMSG
Power rating (P_{PMSG})	6.5 kW
Rated voltage (V_{PMSG}) and current (I_{PMSG})	96 V & 40 A
Stator resistance (R_s) and inductance (L_d, L_q)	5 mΩ, 0.1 mH, 0.1 mH
Peak line-to-line back emf constant ($V_{pk/krpm}$)	290 V/krpm
Pole pairs (p)	12

2.2. Selection criteria and design of basic DC-DC converters

DC-DC converters hold the key role in power delivery and in preserving power as much as possible. In renewable energy applications, these converters are very helpful in improving system efficiency. In this study, the term "basic" is used to describe the DC-DC converters being considered. In general, basic DC-DC converters refer to converters built with a single switch, inductor, and capacitor, such as boost, buck, and buck-boost. However, the term "basic" is expanded based on the following criteria:

- Simple topology: Consists of only one active switch and a total number of active/passive components no greater than six for components consisting of switch, diode, inductor, and capacitor.
- Non-isolated structure: Does not utilize magnetic isolation (i.e., transformers). The input and output share a common electrical ground, which simplifies control and reduces complexity.
- Buck-boost capability: This feature is essential since it has the capability to maintain a consistent output voltage over a wider range of input conditions caused by fluctuating wind speeds, leading to improved energy harvesting efficiency.
- Unidirectional power flow: Power flow only occurs in one direction, from the source (input) to the load (output). In this case, there is no mechanism (either active or passive) that allows power to return to the source.

Various types of DC-DC converters are summarized in Table 3 to be selected as the basic converter candidates. From the selection process, five converters comprising buck-boost, SEPIC, Cuk, zeta, and Luo are suitable for the criteria. The boost converter is also included as the initial converter. Therefore, six basic converters with the circuits shown in Figure 4 were designed. Next, these converters are tested in the SSWT simulation scheme, as demonstrated in Figure 5.

Table 3. Selection process of basic DC-DC converters

DC-DC converter list	Number of components					Non-isolated structure	Buck-boost capability	Unidirectional power flow
	S	D	L	C	Total			
Boost	1	1	1	1	4	✓	×	✓
Quadratic boost	1	3	2	2	8	✓	×	✓
Interleaved boost	2	2	2	1	7	✓	×	✓
Cascaded boost	2	2	2	2	8	✓	×	✓
Buck-boost	1	1	1	1	4	✓	✓	✓
SEPIC	1	1	2	2	6	✓	✓	✓
Modified SEPIC	1	2	2	3	8	✓	✓	✓
Cuk	1	1	2	2	6	✓	✓	✓
Sheppard-Taylor	2	4	2	2	10	✓	✓	✓
Zeta	1	1	2	2	6	✓	✓	✓
Z-source	1	2	2	3	8	✓	×	×
Quasi Z-source	1	1	3	3	8	✓	×	×
Luo	1	2	1	2	6	✓	✓	✓
KY	2	3	1	2	8	✓	✓	✓

*S=Switch, D=Diode, L=Inductor, C=Capacitor

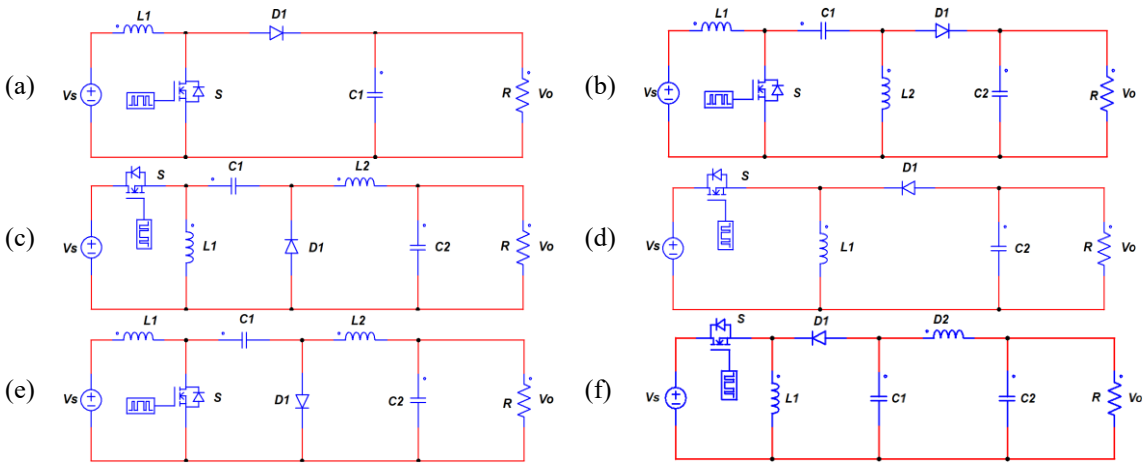

Figure 4. Basic types of DC-DC converters: (a) boost, (b) buck-boost, (c) SEPIC, (d) Cuk, (e) zeta, and (f) Luo

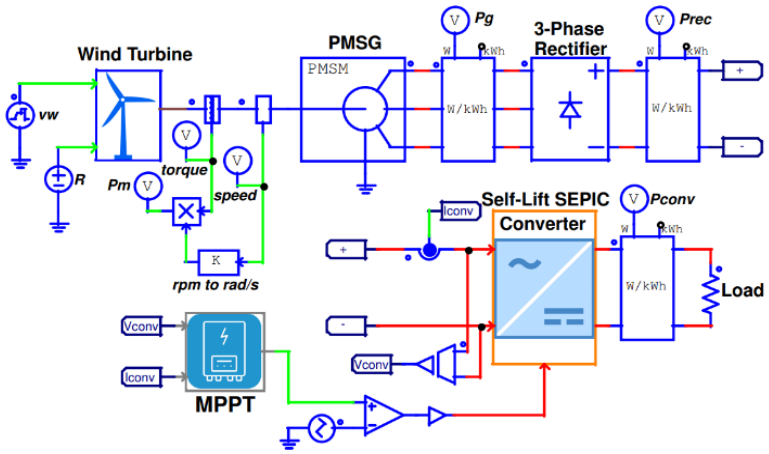

Figure 5. Simulation model of SSWT using PSIM software

Additionally, the converter must be properly designed to match the SSWT capacity, with design specifications calculated according to the guidelines in Table 4 and results summarized in Table 5. V_S is the input voltage or voltage from rectifier (V), V_O is the output voltage, D is the duty cycle, L is inductor value (H), C is capacitor value (F), R is resistive load (Ω), f_s is switching frequency (Hz), ΔiL is inductor current ripple (A), and ΔV_C is capacitor voltage ripple (V). For this design, all converters utilize 10% inductor current ripple, 0.5% voltage ripple, and 25 kHz switching frequency as fundamental design parameters. To closely approximate real operating conditions, parasitic elements are incorporated into the design considerations. The inductor's DC resistance (DCR) serves as the primary factor in calculating inductor losses as given in (7).

$$r_L = k\sqrt{L} = \frac{\rho}{l_{turn}\,A_w}\sqrt{\frac{l_m}{\mu_0\,\mu_r\,A_{tor}}} \tag{7}$$

Where k is a constant with a value of 3.05 to estimate the inductor value by considering variable as follows: ρ is copper resistivity (1.68 x 10^{-8} Ωm), l_{turn} is length of wire per one winding (0.05212 m), A_w is cross sectional area of wire with diameter of 0.5 x 10^{-3} m, μ_0 permeability of vacuum ($4\pi \times 10^{-7}$ H/m), μ_r relative permeability of ferrite (2000), l_m is the magnetic path (0.04712 m), and A_{tor} is cross sectional area of toroid (4 x 10^{-5} m^2). For l_m and A_{tor} can be calculated using (8) and (9), respectively.

$$l_m = 0.5\pi\left(d_{tor\_inner} + d_{tor\_outer}\right) \tag{8}$$

$$A_{tor} = 0.5h_{tor}\left(d_{tor\_outer} - d_{tor\_inner}\right) \tag{9}$$

Where d_{tor_inner} is the inner diameter of the toroid (0.01 m), d_{tor_outer} is the outer diameter of the toroid (0.02 m), and h_{tor} is the height of the toroid (0.008 m). l_{turn} can also be calculated via l_m plus 0.005 as a factor.

For capacitors, the equivalent series resistance (ESR) is considered the dominant contributor to losses, with other parasitic effects being neglected. The capacitor's ESR is determined based on the inductor and capacitor ripple specifications, as formulated in (10). In converters employing dual inductors, the peak currents of both L_1 (I_{L1_peak}) and L_2 (I_{L2_peak}) are accounted for in the design process.

$$r_C = \frac{\Delta V_C}{I_{L1\_peak}+I_{L2\_peak}} = \frac{\Delta V_C}{\left(I_{L1}+\frac{\Delta I_{L1}}{2}\right)+\left(I_{L2}+\frac{\Delta I_{L2}}{2}\right)} \tag{10}$$

The non-ideal behavior of a diode is modeled by its forward voltage drop (V_F) and its effective series resistance (r_D) under forward bias. Here, r_D is treated as a constant parasitic resistance, neglecting the small-signal dynamic resistance that varies with diode current. For the MOSFET switch, the primary non-ideality considered is its on-state resistance (r_{oS}), while higher-order effects like transconductance, junction capacitances, and the body diode are disregarded. Every converter is specified by efficiency that is greatly impacted by component losses, particularly from active and passive components. The common losses in these components are caused by conduction loss specifically in inductor, diode, capacitor, and switch by (11)-(14), respectively. The calculation summary in determining parasitic components is shown in Table 6.

$$P_{loss\_L} = I_{L\_rms}^2\, r_L \tag{11}$$

$$P_{loss\_D} = V_F\, I_{out} + I_{D\_rms}^2\, r_D \tag{12}$$

$$P_{loss\_C} = I_{C\_rms}^2\, r_C \tag{13}$$

$$P_{loss\_S} = P_{cond\_S} + P_{sw\_S} = I_{S\_rms}^2\, r_S + \frac{1}{2} V_{in}\, I_{in}(t_r + t_f) f_s \tag{14}$$

Variable I_{L_rms}, I_{C_rms}, I_{D_rms}, and I_{S_rms} are the root mean square (rms) current of the inductor, diode, capacitor, and switch, respectively. V_F is the forward voltage of the diode (0.7 V), I_{out} is the average output current of the converter, t_r is the rise time of the switching phase, and t_f is the fall time of the switching phase. Finally, the total loss and efficiency of converters are given in (15) and (16), respectively.

$$P_{loss\_tot} = P_{loss\_L} + P_{loss\_D} + P_{loss\_C} + P_{loss\_S} \tag{15}$$

$$\eta = \frac{P_{out}}{P_{in}} \times 100\% = \frac{P_{rec} - P_{loss\_tot}}{P_{rec}} \times 100\% \tag{16}$$

Where P_{rec} is the rectifier output power, which becomes the input power of the converter.

Table 4. Formula to calculate the component of DC-DC converters

Converter Type	Gain	Inductor		Capacitor	
BOOST	$\frac{V_O}{V_S}=\frac{1}{1-D}$	$L_1=\frac{V_S D}{f_s \Delta i L_1}$		$C_1=\frac{V_O D}{f_s \Delta V_O R}$	
BUCK-BOOST	$\frac{V_O}{V_S}=\frac{D}{1-D}$	$L_1=\frac{V_S D}{f_s \Delta i L_1}$		$C_1=\frac{V_O D}{f_s \Delta V_O R}$	
SEPIC	$\frac{V_O}{V_S}=\frac{D}{1-D}$	$L_1=\frac{V_S D}{f_s \Delta i L_1}$	$L_2=\frac{V_S D}{f_s \Delta i L_2}$	$C_1=\frac{V_O D}{f_s \Delta V_{C1} R}$	$C_2=\frac{V_O D}{f_s \Delta V_O R}$
CUK	$\frac{V_O}{V_S}=\frac{D}{1-D}$	$L_1=\frac{V_S D}{f_s \Delta i L_1}$	$L_2=\frac{V_S D}{f_s \Delta i L_2}$	$C_1=\frac{V_S D}{f_s \Delta V_{C1} R}$	$C_2=\frac{V_S D}{8 f_s^2 \Delta V_{C2} L_2}$
ZETA	$\frac{V_O}{V_S}=\frac{D}{1-D}$	$L_1=\frac{V_S D}{f_s \Delta i L_1}$	$L_2=\frac{V_S D}{f_s \Delta i L_2}$	$C_1=\frac{V_O D}{f_s \Delta V_{C1} R}$	$C_2=\frac{V_S D}{8 f_s^2 \Delta V_{C2} L_2}$
LUO	$\frac{V_O}{V_S}=\frac{D}{1-D}$	$L_1=\frac{V_S D}{f_s \Delta i L_1}$	$L_2=\frac{V_S D}{f_s \Delta i L_2}$	$C_1=\frac{V_O D}{f_s \Delta V_{C1} R}$	$C_2=\frac{V_S D}{8 f_s^2 \Delta V_{C2} L_2}$

Table 5. Design result of DC-DC converters

Parameters	Boost	Buck-Boost	SEPIC	Cuk	Zeta	Luo
P_{rat} & R_{rat}	6.5 kW & 30 Ω	6.5 kW & 30 Ω	6.5 kW & 30 Ω	6.5 kW & 30 Ω	6.5 kW & 30 Ω	6.5 kW & 30 Ω
L_1 & L_2	0.9 mH & –	0.8 mH & –	1 mH & 3.5 mH	1 mH & 3.5 mH	1 mH & 3.5 mH	1 mH & 3.5 mH
C_1 & C_2	190 µF & –	210 µF & –	210 µF & 210 µF	210 µF & 4 µF	210 µF & 4 µF	210 µF & 4 µF

Table 6. Parasitic elements of DC-DC converters

Parameters	Boost	Buck-Boost	SEPIC	Cuk	Zeta	Luo
DCR of inductor	r_{L1} = 92 mΩ	r_{L1} = 86 mΩ	r_{L1} = 97 mΩ r_{L2} = 181 mΩ	r_{L1} = 97 mΩ r_{L2} = 181 mΩ	r_{L1} = 97 mΩ r_{L2} = 181 mΩ	r_{L1} = 97 mΩ r_{L2} = 181 mΩ
Forward voltage and diode	V_F = 0.7 V	V_F = 0.7 V	V_F = 0.7 V	V_F = 0.7 V	V_F = 0.7 V	V_F = 0.7 V
on-resistance	r_D = 5 mΩ	r_D = 5 mΩ	r_D = 5 mΩ	r_D = 5 mΩ	r_D = 5 mΩ	r_D = 5 mΩ
ESR of capacitor	r_{C1} = 42 mΩ	r_{C1} = 32 mΩ	r_{C1} = 32 mΩ r_{C2} = 32 mΩ	r_{C1} = 32 mΩ r_{C2} = 32 mΩ	r_{C1} = 32 mΩ r_{C2} = 32 mΩ	r_{C1} = 32 mΩ r_{C2} = 32 mΩ
MOSFET on-resistance	r_{sw} = 5 mΩ	r_{sw} = 5 mΩ	r_{sw} = 5 mΩ	r_{sw} = 5 mΩ	r_{sw} = 5 mΩ	r_{sw} = 5 mΩ

2.3. Concept and design of maximum power point tracking

The application of MPPT techniques plays a fundamental role in maximizing the energy extracted from wind energy conversion systems. In general, MPPT strategies can be classified into two principal approaches: those that regulate the mechanical side to maintain operation along the optimal power–speed characteristic, and those that rely on electrical measurements to identify the maximum power operating point (MPP). Electrical-based approaches are often preferred due to their ability to eliminate complex mechanical control mechanisms. Within this category, several well-established methods include optimal tip speed ratio (OTSR), INC, and P&O techniques [22].

Among the MPPT algorithms, P&O is widely used in PMSG-based wind turbines due to its tracking capability without requiring additional sensors. Additionally, this approach offers further benefits, including reduced system complexity and cost, independence from the need for parameter knowledge, lack of sensitivity, and continuous updates. In a PMSG-based system, the electromagnetic torque generated by the rotor is directly related to the output current, whereas the rotor speed exhibits a proportional relationship with the output voltage. Adjusting the converter's duty cycle enables the observation of voltage variations. By continuously monitoring the output power, the MPPT applies suitable incremental increases or decreases to the duty cycle in the next switching interval to approach the MPP. The algorithm of P&O technique flowchart is shown in Figure 6(a). The logic of P&O algorithm begins with the measurement of the current $I(t)$ and voltage $V(t)$. The instantaneous power $P(t)$ is calculated as the product of $V(t)$ and $I(t)$. The algorithm then computes the differences in voltage ($\Delta V = V(t) - V(t - \Delta T)$) and power ($\Delta P = P(t) - P(t - \Delta T)$) between the current and previous sampling intervals. The decision-making process is as follows:

- If $\Delta P = 0$, the system is assumed to be at the MPP, and no action is taken.
- If $\Delta P > 0$, the algorithm checks the sign of ΔV. If $\Delta V > 0$, the duty cycle D is decreased; otherwise, it is increased.
- If $\Delta P < 0$, the algorithm also checks ΔV. If $\Delta V > 0$, D is increased; otherwise, it is decreased.

This iterative process ensures that the operating point moves toward the MPP by continuously adjusting D based on the observed changes in P and V.

Another widely used technique, called INC, has been recognized as the optimal approach grounded in the disturbance and observation principle. This method combines notable benefits, including a quick and efficient response. Moreover, INC can maintain convergence speed and steady state error, which becomes the

main limitation in P&O method. The algorithm of the INC technique is shown in Figure 6(b). The INC algorithm leverages the relationship between the instantaneous conductance (I/V) and the incremental conductance ($\Delta I/\Delta V$) to track the MPP. The algorithm starts by measuring $I(t)$ and $V(t)$, then calculates the differences $\Delta I = I(t) - I(t - \Delta T)$ and $\Delta V = V(t) - V(t - \Delta T)$. The decision logic is as follows:

- If $\Delta V = 0$, the algorithm checks ΔI. If $\Delta I = 0$, the system is at the MPP. If $\Delta I > 0$, D is decreased; otherwise, it is increased.
- If $\Delta V \neq 0$, the algorithm compares $\Delta I/\Delta V$ to $-I/V$. If $\Delta I/\Delta V = -I/V$, the MPP is reached. If $\Delta I/\Delta V > -I/V$, D is decreased; otherwise, it is increased.

The INC algorithm is more precise than P&O because it uses the derivative of power with respect to voltage (dP/dV) to determine the direction of perturbation, minimizing oscillations around the MPP. Once the MPP is attained, the INC stabilizes and ceases to fluctuate around the operating point [23]. However, it is essential to note that INC has limitations, particularly in the complex calculation of derivatives, and its speed in reaching the MPP is influenced by the offset of ΔV.

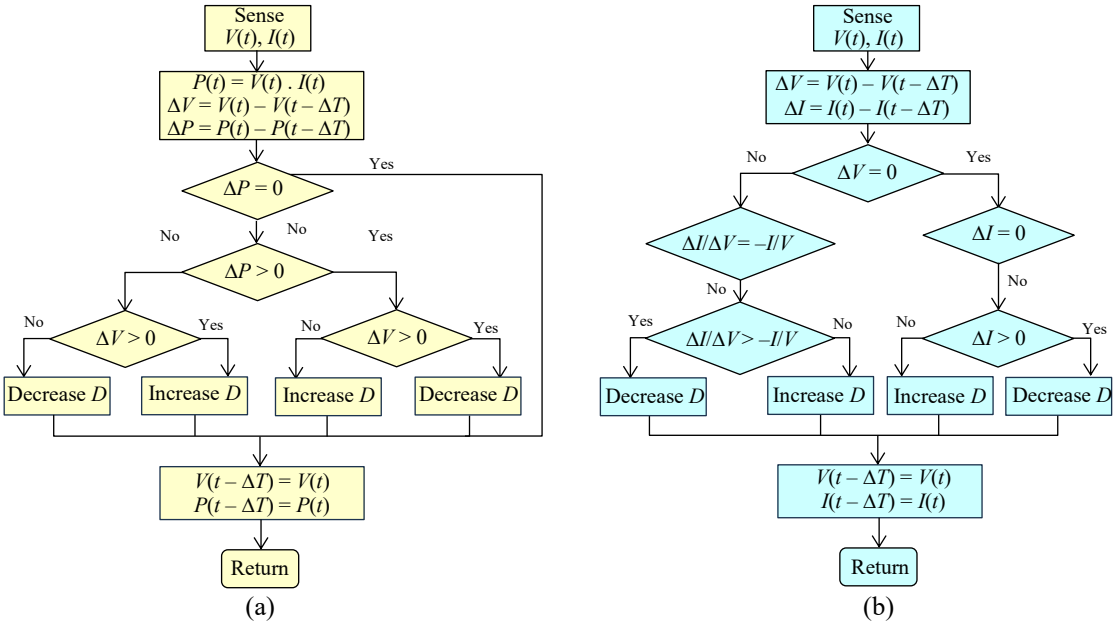

Figure 6. The concept and workflow of (a) P&O method and (b) INC method

3. RESULTS AND DISCUSSION

3.1. Power extraction characteristic for SSWT

In the examination of power extraction, the SSWT was subjected to testing at different wind speeds employing basic DC-DC converter topologies. Here, power extraction is defined as the net electrical power successfully delivered by the overall system, measured at the load side after the power electronics devices, particularly DC-DC converters in this context. This power highlights the role of both the converter and the MPPT strategy in determining the effective energy utilization of the turbine. Converters were assessed for their role in power extraction in SSWT along with the implementation of P&O and INC for power maximizing strategy as shown in Figures 7(a) and 7(b), respectively. It is evident that as wind speed increases, power extraction significantly rises, following an exponential trend. Generally, both P&O and INC produce similar optimal power, and the SSWT employing the boost converter consistently achieves the highest power extraction, whereas the Luo converter demonstrates the lowest. For instance, at a rated wind speed of 12 m/s, the Boost converter yields nearly 5,650 W with P&O and 5,633 W with INC, while the Luo converter produces only around 4,752 W and 4,762 W, respectively. Other converters such as buck-boost, SEPIC, Cuk, and zeta present intermediate performance values between these two extremes.

Nevertheless, power extraction should also be interpreted in relation to the cut-in speed ability, as depicted in the left panels of Figures 7(a) and 7(b). Under P&O, the Boost converter shows the highest cut-in speed at 5.6 m/s, while the Luo converter achieves the lowest at 4.1 m/s. A similar pattern is found with INC, where boost requires 5.5 m/s to initiate power generation, while Luo starts as early as 4.0 m/s. This characteristic indicates that a lower cut-in speed is preferable, since the SSWT can already generate electricity at relatively weak wind conditions. Therefore, while the boost converter provides superior maximum power at high wind speeds, the Luo converter offers better performance at low wind speeds due to its ability to harvest

energy earlier. This trade-off implies that the most suitable converter topology should be selected not only on the basis of peak power capability but also considering operability under low-wind scenarios. It also highlights that Boost converter has narrow wind speed range compared to the other five converters, while Luo shows a wider range since it can convert power at very low wind speed.

Additionally, under dynamic wind conditions, all converters successfully extract the available wind power, as illustrated in Figure 8. This finding highlights the capability of each converter topology to maintain reliable operation even when subjected to fluctuating wind speeds. The comparative power extraction rates of the tested basic converters further demonstrate their compatibility with the implemented MPPT methods. The consistency in performance across converters indicates that both P&O and INC algorithms are effective in tracking the MPP, regardless of the converter type. This observation not only validates the robustness of the MPPT strategies but also confirms the technical feasibility of integrating these basic converter topologies into wind energy systems. Similar conclusions were also emphasized in [15], [21].

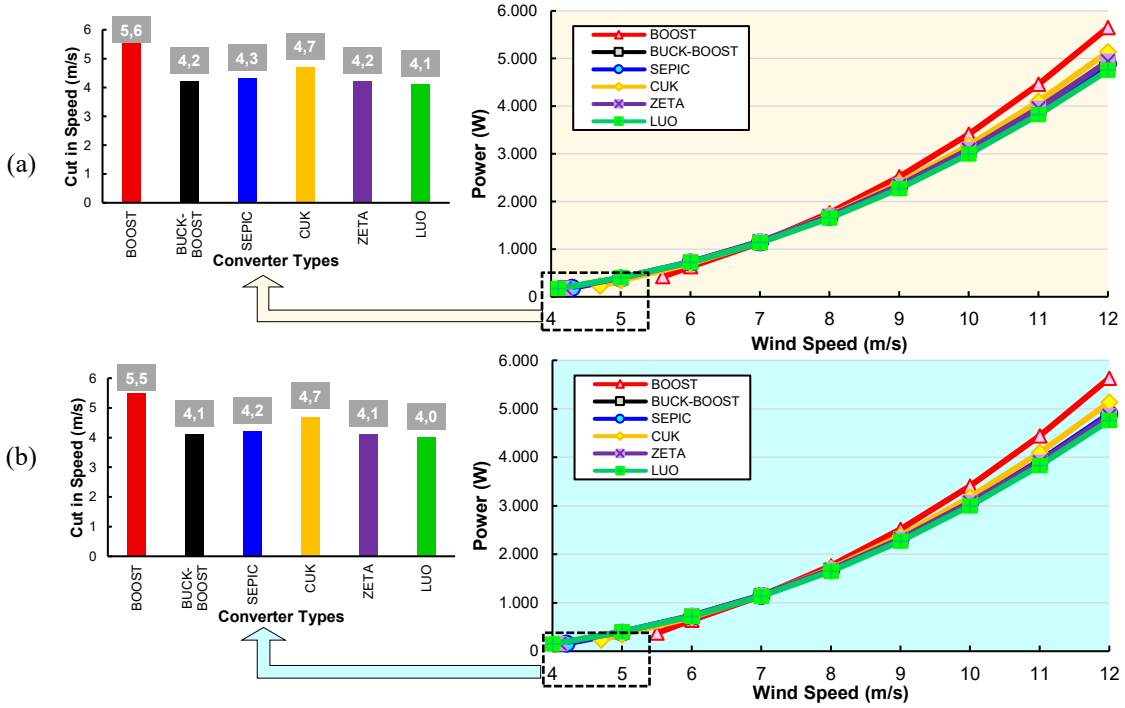

Figure 7. Power extraction and cut-in wind speed profile of SSWT for all basic DC-DC converters at different wind speed: (a) using MPPT P&O and (b) using MPPT INC

3.2. Comparison of MPPT performance

The MPPT efficiency profiles of the examined converters under P&O and INC strategies are presented in Figures 9(a) and 9(b), respectively. In general, both algorithms demonstrate a rapid increase in efficiency as wind speed rises, with performance stabilizing above 90% once the wind speed exceeds approximately 5–6 m/s. However, the exact wind speed range over which high efficiency is maintained differs across converter topologies. The boost converter achieves MPPT efficiency consistently above 90% between 6 m/s and 12 m/s. In contrast, the remaining five converters display more variable ranges: Buck-Boost, SEPIC, and ZETA maintain above 90% efficiency from around 5–10 m/s, Cuk from 6–11 m/s, and Luo from 5–9 m/s. These ranges indicate that while all converters are capable of high efficiency, their stability across the full spectrum of wind speeds differs significantly.

The observed variations can be attributed to both converter topology and algorithmic interaction with the nonlinear power curve of the SSWT. Boost benefits from its higher voltage conversion ratio and simpler power transfer path, which help to maintain stable MPPT tracking over a wider operating region [24]. Furthermore, in this setting, the incremental slope information used by INC offers little systematic benefit over the well-tuned P&O perturbations. It is evidenced by the average MPPT efficiency of P&O consistently surpasses INC for almost all converters. In detail, for P&O method, the converters can be ranked as boost > buck-boost > zeta > SEPIC > Luo > Cuk, with boost consistently exceeding 92% average MPPT efficiency and Cuk showing the lowest performance at only almost 90%. In contrast, when INC is applied, the ranking

slightly shifts to boost > Cuk > buck-boost > zeta > Luo > SEPIC, where Cuk improves its relative position, although its overall efficiency remains below that of the leading converters. SEPIC surprisingly falls into the lowest efficiency for the INC strategy. These orders show the natural characteristics of each topology, which are affected by the impact of energy transfer in inductors and capacitors, voltage distribution, and control sensitivity to respond to every change during peak tracking. In short, while algorithmic differences are marginal, the converter topology itself is the dominant factor in determining how effectively the SSWT's variable power is harvested [25].

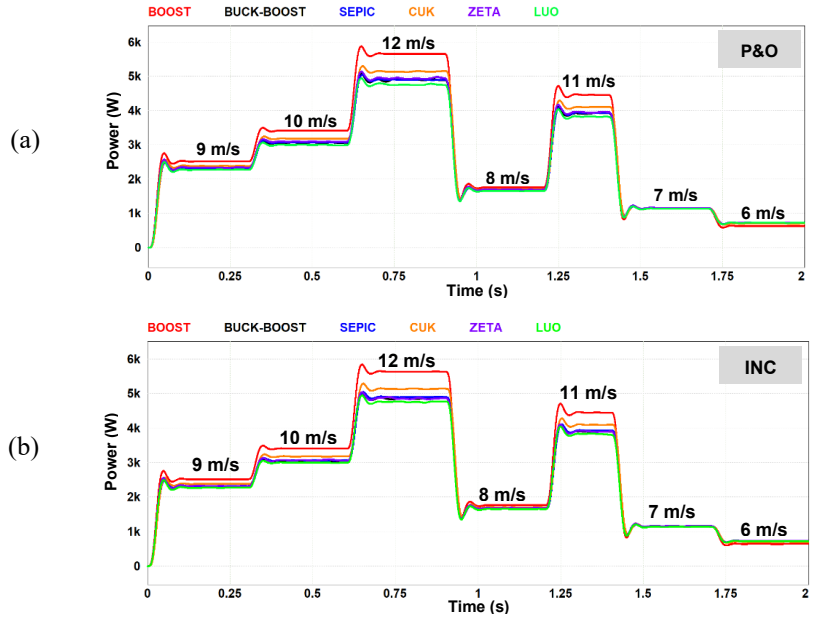

Figure 8. Power extraction profile for all converters under dynamic conditions by using (a) P&O and (b) INC

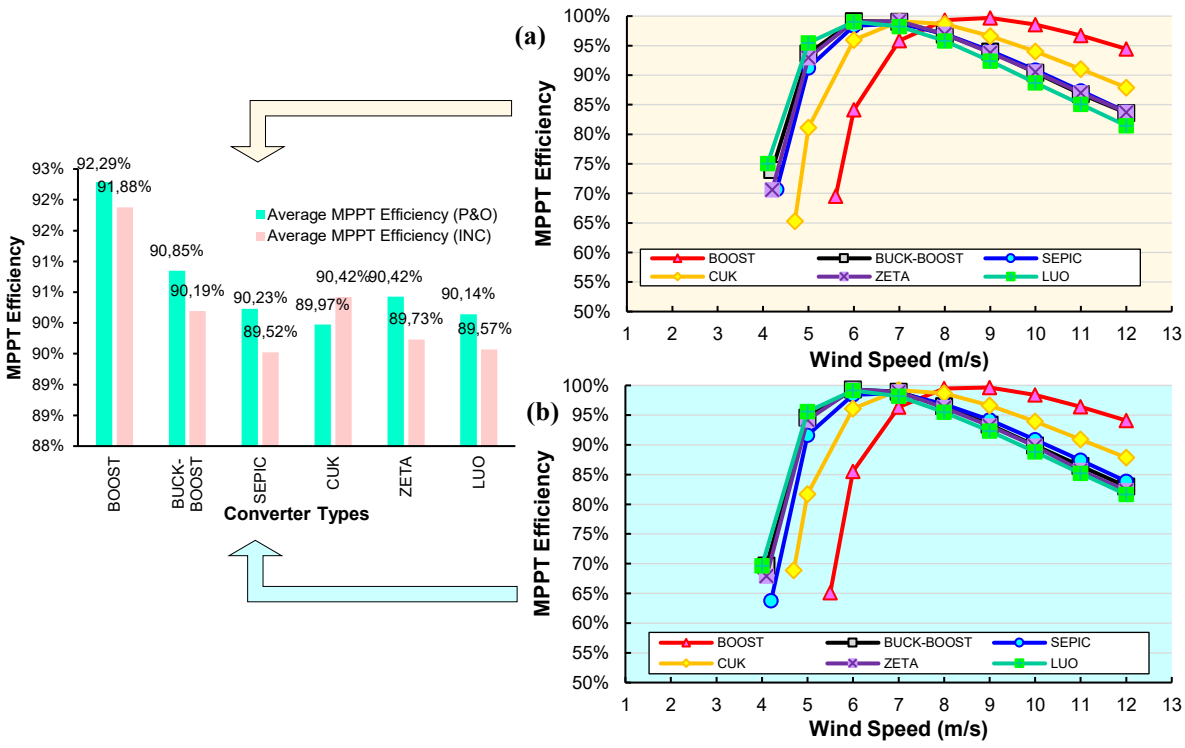

Figure 9. MPPT efficiency at different wind speed by using (a) P&O and (b) INC

3.3. Properties comparison of basic DC-DC converters

In a detailed scrutiny, the performance of converters can be analyzed through various parameters such as voltage gain, efficiency, voltage stress, current stress, and losses. The first assessment is to check the comparison of voltage gain among all converters as depicted in Figure 10. This comparison is done by setting duty cycle variation with an input voltage of 130 V serving as the rectifier output voltage and involves the parasitic elements in each converter. The boost converter exhibits higher voltage gain across all duty cycle ranges compared to the five other converters. As the duty cycle increases, the voltage gain exponentially rises to a duty cycle of 0.9, reaching a maximum gain close to 7. In contrast, the other five converters exhibit very similar voltage gain characteristics since their voltage gain equations share the same dependency on the duty cycle, albeit with different circuit topologies and additional components. In detail, observing the voltage gain at the highest duty cycle, the boost converter exhibits the highest performance, whereas the Luo converter records the lowest. Meanwhile, the buck-boost, SEPIC, Cuk, and Zeta converters, however, exhibit relatively similar voltage gain profiles. The presence of parasitic elements incorporated in the simulation moderately affects the overall gain but maintains the relative ranking among the converters. It is worth noting that in ideal conditions, the boost converter can achieve voltage gains as large as 10 to 12 times the input voltage at high duty cycles [26], [27]. However, when non-ideality conditions are included, the practical voltage gain is significantly reduced due to the inherent resistances of the composing devices and energy dissipation during switching transitions. This explains why the observed maximum gain hovers around 7 rather than reaching the ideal theoretical values, providing a more realistic of converter performance.

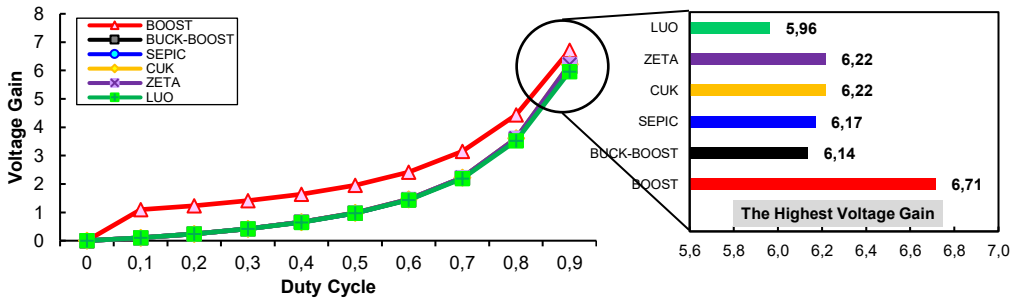

Figure 10. Voltage gain comparison for all basic DC-DC converters

The second important criterion to assess the converters is efficiency, which is measured across different wind speeds using both P&O (Figure 11(a)) and INC (Figure 11(b)) strategies. By considering non-ideal components, all converters show efficiencies above 90%, with the boost converter still dominating as the highest. This converter can reach values close to 94%, although it covers only a narrow wind speed range. This superior performance can be linked to the boost converter's simpler power stage and lower conduction losses relative to other topologies. Following the boost, zeta converter shows the next-best efficiency around 92% to 93%, while the buck-boost, SEPIC, Cuk, and Luo converters demonstrate similar efficiencies slightly above 91%. For both MPPT strategies, Cuk consistently exhibits the lowest average efficiency.

When comparing the two MPPT algorithms, P&O and INC, the relative ranking of converters reveals subtle but important differences. Under the P&O method, the boost converter achieves the highest average efficiency, followed by zeta, buck-boost, and Luo, while SEPIC and Cuk remain clustered closely together and consistently perform the worst. In contrast, the INC method shows a similar order, but this algorithm provides a relatively higher efficiency improvement for almost all converters compared to P&O. These results confirm that the boost converter is universally the most effective across both MPPT techniques, and INC can improve converter efficiency. It is worth noting that the efficiency profile between MPPT extraction (measured at the input side of the converter) and converter efficiency (measured at the output side of the converter) shows significant differences in order due to additional power losses inside the converter components, which alter the overall ranking compared to the extracted input power.

A more detailed evaluation of converter performance can be drawn from the loss values as shown in Figure 12(a). The result is similar to the efficiency profile in which boost converter shows the lowest losses, competing with Zeta, while the four remaining converters follow the same order, with Cuk exhibiting the highest power losses, reaching nearly 200 W. This result is not always aligned with the voltage stress as shown in Figure 12(b), where Cuk has the lowest voltage stress after boost, yet still records the highest total losses. This condition seems contradictory, but it is expected that the most influential variable in the loss calculation is the square of the current and component non-ideality. It is evidenced by the current stress profile in Figure 12(c) that has quite similar order to the power loss result of Cuk.

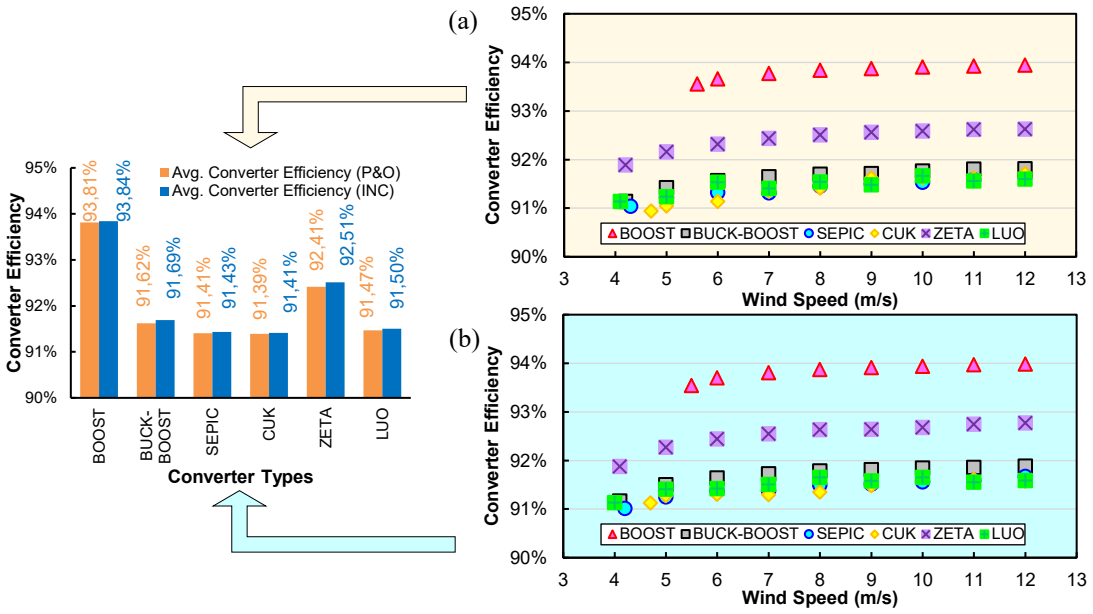

Figure 11. Converter's efficiency for all basic DC-DC converters by using (a) P&O and (b) INC

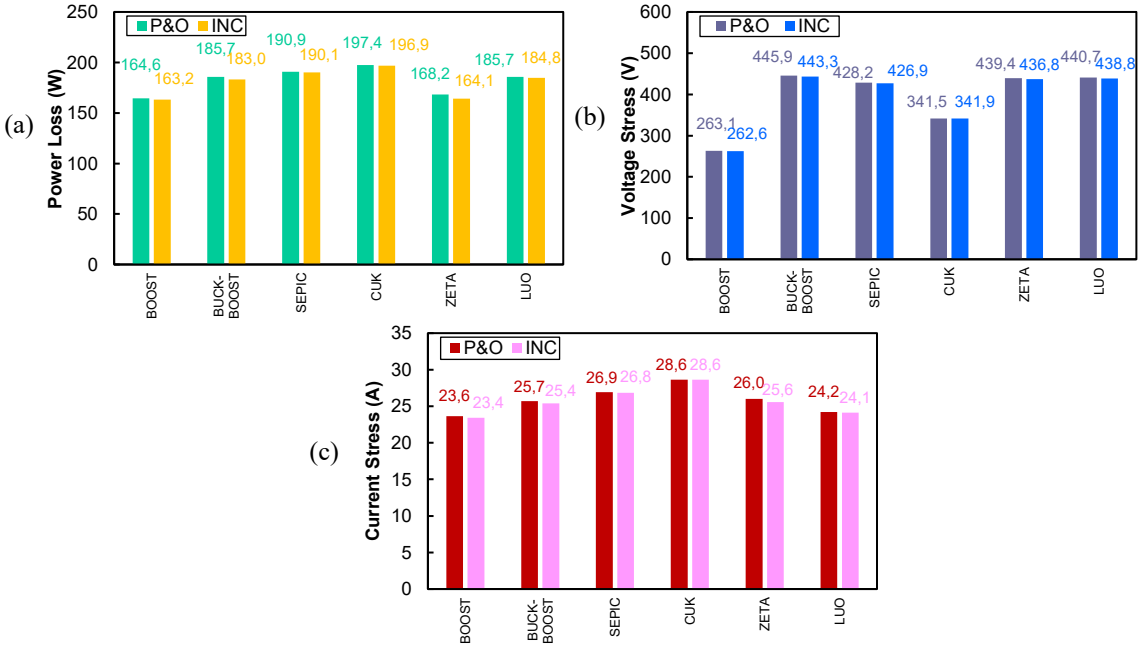

Figure 12. Comparison of converter properties: (a) power loss, (b) voltage stress, and (c) current stress

Additionally, the loss contribution of each component can be seen in Figure 13. Overall, the percentage distribution of losses is similar for both MPPT methods when applied to the same converter. In detail, across these MPPT strategies, the inductor is the dominant source of loss, particularly for single-inductor converters such as boost and buck-boost converters. Inductor losses are significant, reaching nearly 50% of the total. In contrast, SEPIC, Cuk, zeta, and Luo converters, which utilize dual inductors, exhibit the highest losses in the MOSFET due to conduction and switching effects. These losses are slightly higher than inductor losses, with both components contributing nearly 80% of the total converter losses. This result is interesting because dual-inductor converters have more winding resistance, yet the current is shared between the two inductors, making the effective current in each smaller than in single-inductor converters. Since inductor loss is proportional to the square of the current, this current sharing leads to a significant reduction in inductor-related losses. Furthermore, capacitor losses remain relatively minor in all converters, generally below 5%, regardless

of whether single or multiple capacitors are used. These losses are primarily due to conduction, as the actual current through the capacitor is very small. Diode losses, meanwhile, are governed by forward voltage drop and the diode's internal resistance, contributing around 8–12% of the total losses.

After obtaining the efficiency profile, the final efficiency of the SSWT for all converters under the P&O and INC techniques can be determined. This efficiency is measured at the converter output (load) relative to the maximum available wind power, and the results are shown in Figure 14. The SSWT with the Boost converter remains the most optimal, followed by zeta, buck-boost, Luo, Cuk, and SEPIC. It is also noted that P&O is more suitable to be applied compared to INC, since it enables the converter to achieve higher power extraction. These findings provide valuable insights for selecting appropriate converter topologies and MPPT strategies in future SSWT applications.

The overall performance of selected basic DC-DC converters is illustrated in Figure 15 using radar charts. These charts evaluate key aspects, including power extraction, wind speed range, MPPT efficiency, converter efficiency, power loss, voltage gain, voltage stress, and current stress, with each aspect rated on a scale from 1 to 6. Based on this assessment, the boost converter is strongly recommended for use as a DC-DC converter in SSWT applications, as it demonstrates superior performance across most criteria. Its primary limitation is the narrow wind speed range, which may restrict its applicability in variable wind conditions. As an alternative, a step-up/step-down type, such as the zeta converter, can be considered, given its competitive performance relative to the Boost converter and its advantage of a broader wind speed range, enabling more robust operation in fluctuating environments. In contrast, the SEPIC converter is not recommended, owing to its consistently low scores across multiple aspects, which indicate suboptimal efficiency and higher stresses.

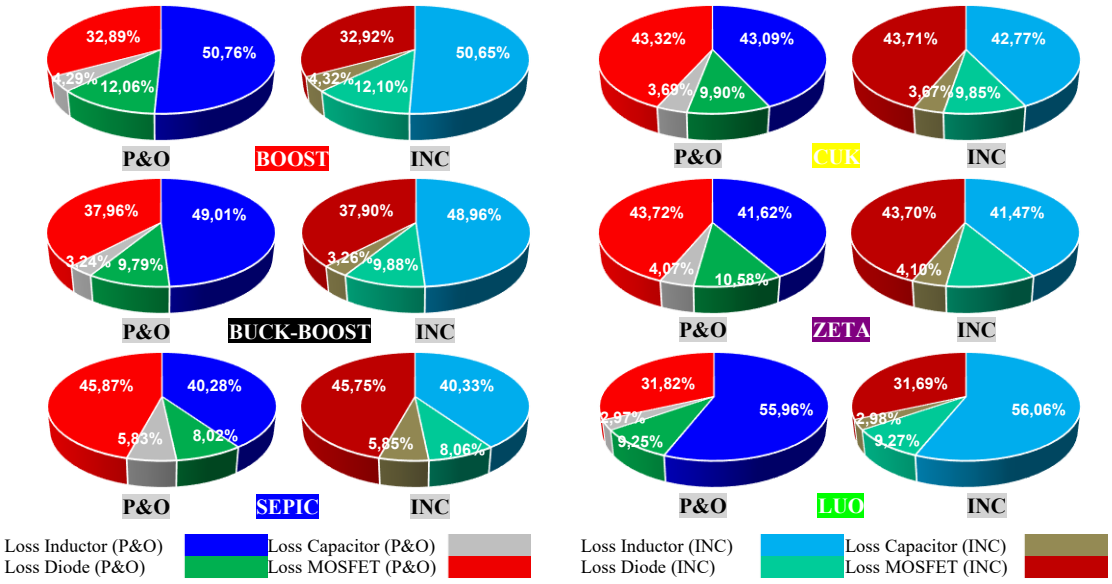

Figure 13. Comparison of detailed losses for all converters under P&O and INC

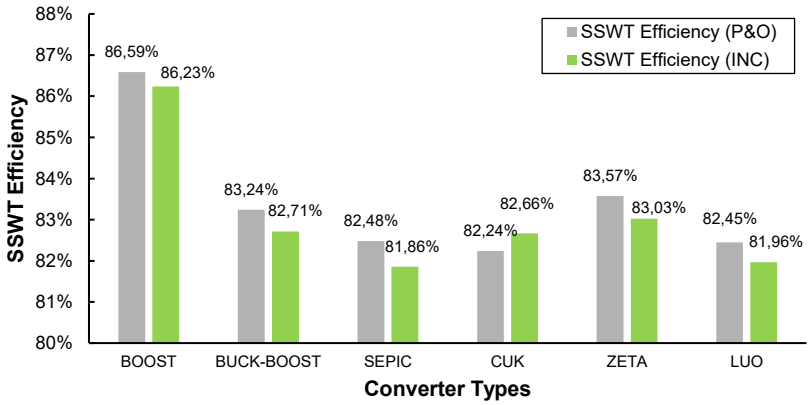

Figure 14. SSWT efficiency for all basic DC-DC converters using P&O and INC

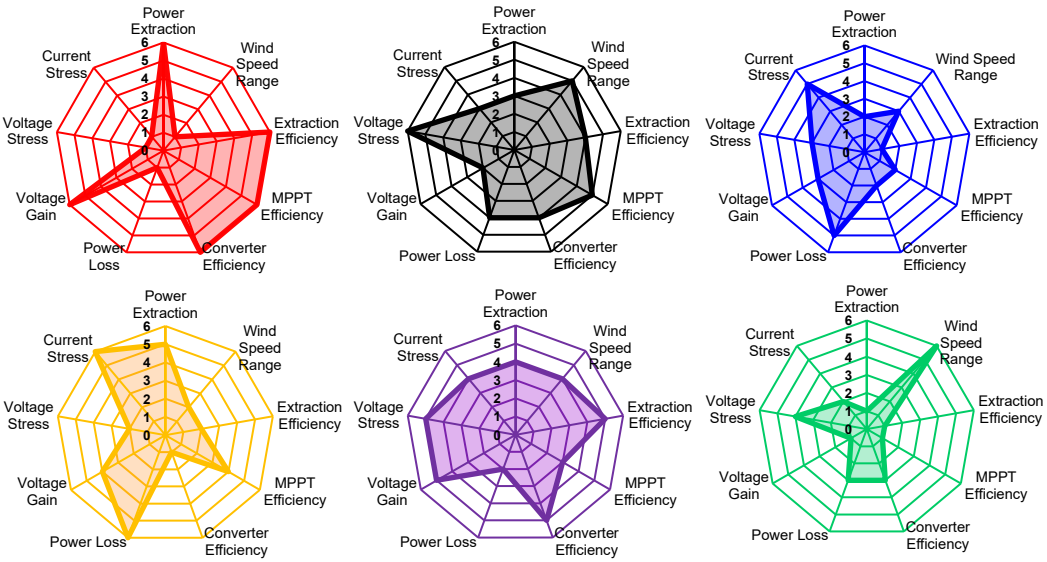

Figure 15. Comparison of converter overall performance with radar chart: boost (red), buck-boost (black), SEPIC (blue), Cuk (orange), zeta (purple), and Luo (green)

4. CONCLUSION

An extensive investigation was carried out to analyze the performance of a SSWT with basic types of DC-DC converters employed. A selection process was conducted to choose the converters based on topology simplicity, non-isolated structure, buck-boost capability, and unidirectional power flow, in which six converters comprising boost, buck-boost, SEPIC, Cuk, zeta, and Luo were considered. These converters were implemented in a 6.5 kW SSWT system with the configuration consisting of a wind turbine, PMSG, rectifier, DC-DC converter, MPPT technique, and load. A comprehensive assessment was conducted to evaluate the performance of each converter in the SSWT. Some criteria, including power extraction, wind speed range, MPPT efficiency, converter efficiency, power loss, voltage gain, voltage stress, and current stress, were considered. Moreover, the assessment was performed under two MPPT strategies, i.e., P&O and INC. In the converter design, a non-ideality factor was also included to achieve a more realistic condition. Through experiments conducted at varying wind speeds, the boost converter was able to extract the highest power (up to 5.6 kW), MPPT efficiency (up to 92%), and converter efficiency (up to 93%) in both MPPT strategies, although it was limited to a narrow wind speed range. The boost converter was also superior in other converter parameters, achieving the highest voltage gain and lowest power loss, voltage stress, and current stress. As an alternative, the zeta converter was also recommended in SSWT applications since its performance was competitive with the boost converter while providing a broader wind speed range. Along with zeta, the buck-boost converter is considerable since it offers a voltage regulation ability which cannot be found in the boost converter. However, both converters pose quite high voltage and current stresses, which may require costly MOSFET components in the application. SEPIC and Cuk, the sibling converters, are not recommended for SSWT since their overall performance is low, while the Luo converter, as an intermediate converter, may be useful for low-wind-speed applications. In the future, the selection of basic DC-DC converters needs to be proven in hardware tests to evaluate their effectiveness in real SSWT applications. Moreover, the development of advanced MPPT methods to maximize power extraction and the application of soft-switching techniques to improve converter efficiency are necessary for well-established SSWT systems.

ACKNOWLEDGMENTS

The authors wish to convey their heartfelt appreciation to Universitas Brawijaya for their generous support in providing essential research facilities that enabled the completion of this work.

FUNDING INFORMATION

This research was funded by Universitas Brawijaya through the Professor and Doctor Research Grant Program 2023 (Grant No. 18/UN10/PN/2023).

AUTHOR CONTRIBUTIONS STATEMENT

This journal uses the Contributor Roles Taxonomy (CRediT) to recognize individual author contributions, reduce authorship disputes, and facilitate collaboration.

Name of Author	C	M	So	Va	Fo	I	R	D	O	E	Vi	Su	P	Fu
Rizki Mendung Ariefianto	✓	✓	✓	✓	✓	✓		✓	✓	✓	✓		✓	
Rini Nur Hasanah	✓	✓			✓	✓	✓	✓	✓	✓		✓	✓	✓
Hadi Suyono	✓						✓			✓			✓	✓
Tri Nurwati		✓	✓		✓					✓	✓			
Eduard Muljadi	✓				✓		✓			✓		✓		
Hazlie Mokhlis					✓		✓			✓		✓		✓

C : **C**onceptualization
M : **M**ethodology
So : **So**ftware
Va : **Va**lidation
Fo : **Fo**rmal analysis
I : **I**nvestigation
R : **R**esources
D : **D**ata Curation
O : Writing - **O**riginal Draft
E : Writing - Review & **E**diting
Vi : **Vi**sualization
Su : **Su**pervision
P : **P**roject administration
Fu : **Fu**nding acquisition

CONFLICT OF INTEREST STATEMENT

The authors declare no conflict of interest.

DATA AVAILABILITY

This study did not involve the creation or analysis of new datasets; thus, data availability is not applicable.

REFERENCES

[1] P. Paiboonsin, G. Oluleye, M. Howells, R. Yeganyan, C. Cannone, and S. Patterson, "Pathways to clean energy transition in Indonesia's electricity sector with open-source energy modelling system modelling (OSeMOSYS)," *Energies*, vol. 17, no. 1, p. 75, 2024, doi: 10.3390/en17010075.

[2] P. Sadorsky, "Wind energy for sustainable development: driving factors and future outlook," *Journal of Cleaner Production*, vol. 289, p. 125779, Mar. 2021, doi: 10.1016/j.jclepro.2020.125779.

[3] A. Bensalah, G. Barakat, and Y. Amara, "Electrical generators for large wind turbine: trends and challenges," *Energies*, vol. 15, no. 18, p. 6700, Sep. 2022, doi: 10.3390/en15186700.

[4] M. Bošnjaković, M. Katinić, R. Santa, and D. Marić, "Wind turbine technology trends," *Applied Sciences*, vol. 12, no. 17, p. 8653, Aug. 2022, doi: 10.3390/app12178653.

[5] N. A. Pambudi *et al.*, "Renewable energy in Indonesia: current status, potential, and future development," *Sustainability*, vol. 15, no. 3, p. 2342, Jan. 2023, doi: 10.3390/su15032342.

[6] B. Desalegn, D. Gebeyehu, and B. Tamirat, "Wind energy conversion technologies and engineering approaches to enhancing wind power generation: a review," *SSRN Electronic Journal*, 2022, doi: 10.2139/ssrn.4049719.

[7] H. Han *et al.*, "Design of a parallel all-DC wind power system with turbine-side boost based on a new DC conversion," *IEEE Access*, vol. 12, pp. 3054–3069, 2024, doi: 10.1109/ACCESS.2023.3349294.

[8] A. J. Balbino, B. D. S. Nora, and T. B. Lazzarin, "An improved mechanical sensorless maximum power point tracking method for permanent-magnet synchronous generator-based small wind turbines systems," *IEEE Transactions on Industrial Electronics*, vol. 69, no. 5, pp. 4765–4775, 2022, doi: 10.1109/TIE.2021.3084176.

[9] S. Pranupa, A. T. Sriram, and S. N. Rao, "Wind energy conversion system using perturb & observe-based maximum power point approach interfaced with t-type three-level inverter connected to grid," *Clean Energy*, vol. 6, no. 4, pp. 534–549, 2022, doi: 10.1093/ce/zkac034.

[10] S. S. Khan and H. Wen, "A comprehensive review of fault diagnosis and tolerant control in DC-DC converters for DC microgrids," *IEEE Access*, vol. 9, pp. 80100–80127, 2021, doi: 10.1109/ACCESS.2021.3083721.

[11] A. Zentani, A. Almaktoof, and M. T. E. Kahn, "DC-DC boost converter with PO MPPT applied to a stand-alone small wind turbine system," in *Proceedings - 30th Southern African Universities Power Engineering Conference, SAUPEC 2022*, 2022, doi: 10.1109/SAUPEC55179.2022.9730744.

[12] R. D. N. Aditama, N. Ramadhani, T. Ardriani, J. Furqani, A. Rizqiawan, and P. A. Dahono, "New modular multilevel dc–dc converter derived from modified buck–boost dc–dc converter," *Energies*, vol. 16, no. 19, 2023, doi: 10.3390/en16196950.

[13] R. I. Putri, M. Pujiantara, A. Priyadi, T. Ise, and M. H. Purnomo, "Maximum power extraction improvement using sensorless controller based on adaptive perturb and observe algorithm for PMSG wind turbine application," *IET Electric Power Applications*, vol. 12, no. 4, pp. 455–462, 2018, doi: 10.1049/iet-epa.2017.0603.

[14] I. H. D. N. Oliveira and N. Silva, "Maximum power point tracking of a wind generator using a SEPIC converter with LMI control," in *14th Brazilian Power Electronics Conference, COBEP 2017*, 2017, pp. 1–7, doi: 10.1109/COBEP.2017.8257306.

[15] R. Syahputra and I. Soesanti, "Performance improvement for small-scale wind turbine system based on maximum power point tracking control," *Energies*, vol. 12, no. 20, 2019, doi: 10.3390/en12203938.

[16] H. El Aissaoui, A. El Ougli, and B. Tidhaf, "Neural networks and fuzzy logic based maximum power point tracking control for wind energy conversion system," *Advances in Science, Technology and Engineering Systems Journal*, vol. 6, no. 2, pp. 586–592, 2021, doi: 10.25046/aj060267.

[17] A. Watil, A. El Magri, R. Lajouad, A. Raihani, and F. Giri, "Multi-mode control strategy for a stand-alone wind energy conversion system with battery energy storage," *Journal of Energy Storage*, vol. 51, 2022, doi: 10.1016/j.est.2022.104481.
[18] S. Tounsi, "Innovative maximum power point tracking technique for wind energy conversion system," *Wind Engineering*, vol. 48, no. 3, pp. 384–407, 2024, doi: 10.1177/0309524X231201656.
[19] M. Q. Nawaz, W. Jiang, and A. Khan, "Enhancing wind turbine stability and performance: a case study on speed control and maximum power point tracking," *Diyala Journal of Engineering Sciences*, vol. 17, no. 1, pp. 1–18, 2024, doi: 10.24237/djes.2024.17101.
[20] M. K. Saifullah, E. Jahan, and M. N. Uddin, "MPPT control for standalone wind energy conversion system: integrating hybrid P&O and ANN with voltage-lift boost converter," in *7th International Conference on Development in Renewable Energy Technology, ICDRET 2024*, 2024, doi: 10.1109/ICDRET60388.2024.10503626.
[21] S. Sri Ragavi and G. Emayavaramban, "Performance analysis of permanent magnet synchronous generator with wind energy converters," in *Proceedings - 2024 5th International Conference on Mobile Computing and Sustainable Informatics, ICMCSI 2024*, 2024, pp. 870–876, doi: 10.1109/ICMCSI61536.2024.00137.
[22] H. H. H. Mousa, A. R. Youssef, and E. E. M. Mohamed, "Variable step size P&O MPPT algorithm for optimal power extraction of multi-phase pmsg based wind generation system," *International Journal of Electrical Power and Energy Systems*, vol. 108, pp. 218–231, 2019, doi: 10.1016/j.ijepes.2018.12.044.
[23] D. A. Asoh, B. D. Noumsi, and E. N. Mbinkar, "Maximum power point tracking using the incremental conductance algorithm for pv systems operating in rapidly changing environmental conditions," *Smart Grid and Renewable Energy*, vol. 13, no. 05, pp. 89–108, 2022, doi: 10.4236/sgre.2022.135006.
[24] H. Hussein, A. Mahdi, and T. Abdul-Wahhab, "Design of a boost converter with MPPT algorithm for a PV generator under extreme operating conditions," *Engineering and Technology Journal*, vol. 39, no. 10, pp. 1473–1480, 2021, doi: 10.30684/etj.v39i10.1888.
[25] A. Mansouri, A. El Magri, R. Lajouad, I. El Myasse, E. K. Younes, and F. Giri, "Wind energy based conversion topologies and maximum power point tracking: a comprehensive review and analysis," *e-Prime - Advances in Electrical Engineering, Electronics and Energy*, vol. 6, 2023, doi: 10.1016/j.prime.2023.100351.
[26] H. Gholizadeh, R. Sharifi Shahrivar, M. R. Hashemi, E. Afjei, and S. A. Gorji, "Design and implementation a single-switch step-up DC-DC converter based on cascaded boost and Luo converters," *Energies*, vol. 14, no. 12, 2021, doi: 10.3390/en14123584.
[27] H. Gholizadeh, R. S. Shahrivar, S. Amini, and T. Rahimi, "An improved cascaded boost converter with an ultra-high voltage gain suitable for dielectric quality tests," *Energies*, vol. 17, no. 15, 2024, doi: 10.3390/en17153861.

BIOGRAPHIES OF AUTHORS

Rizki Mendung Ariefianto was born in Lumajang, Indonesia. He received a B.Eng. degree in electrical engineering from Institut Teknologi Sepuluh Nopember, Indonesia, in 2018, and two M.Eng. degrees in ocean engineering from Institut Teknologi Sepuluh Nopember, Indonesia, in 2020 and electrical power engineering from Universitas Brawijaya, Indonesia, in 2022. He has been with the Department of Electrical Engineering, Universitas Brawijaya, Indonesia, as a lecturer/researcher since March 2023. His research interests include distributed generation, power electronics, power systems optimization, solar power systems, turbine study, feasibility study of renewable energy, and power system control. He can be contacted at email: rizki.mendung.a@ub.ac.id.

Rini Nur Hasanah was born in Yogyakarta, Indonesia. She received a B.Eng. degree in electrical engineering from Institut Teknologi Bandung, Indonesia, in 1994, the M.Sc. degree in energy studies from Ecole Polytechnique Federale de Lausanne, Switzerland, in 2001, and the Ph.D. degree in electromechanics from Ecole Polytechnique Federale de Lausanne, Switzerland, in 2005. Her major research interests include electric machinery, power system engineering, power electronics and electric drives, and renewable energy development and management. She joined the Department of Electrical Engineering, Faculty of Engineering, Universitas Brawijaya, as a lecturer/researcher in 1995 and is currently a professor in electrical energy and power engineering. She can be contacted at email: rini.hasanah@ub.ac.id.

Hadi Suyono was born in Pamekasan, Indonesia, on May 20, 1973. He received the bachelor degree in electrical engineering from the Department of Electrical Engineering, Universitas Brawijaya, Malang, Indonesia, in 1996, the M.Eng. degree in electrical engineering from Universitas Gadjah Mada, Yogyakarta, Indonesia, in 2000, and the Ph.D. degree in electrical power system engineering from the University of Malaya, Kuala Lumpur, Malaysia, in 2006. His major research interests include power system engineering, artificial intelligence, and renewable energy. He joined the Department of Electrical Engineering, Faculty of Engineering, Universitas Brawijaya, as a lecturer/researcher in 2008 and is currently a professor in electrical power system and artificial intelligence. He currently serves as Dean of the Faculty of Engineering, Universitas Brawijaya. He can be contacted at email: hadis@ub.ac.id.

Tri Nurwati was born in Malang, Indonesia, on June 15th, 1979. She finished her undergraduate study in electronics engineering at Universitas Brawijaya, Indonesia, postgraduate master's degree in control engineering at Institut Teknologi Sepuluh Nopember, Indonesia, and doctoral degree in electrical engineering at the University of Picardie Jules Verne, France, consecutively in 2002, 2004, and 2019. She has been with the Electrical Engineering Department of Universitas Brawijaya, Indonesia, as a lecturer/researcher since December 2008. She currently serves as the Head of the Power Electronics Laboratory of Universitas Brawijaya. Her research interests include electrical engineering, control engineering, power electronics and drives, and renewable energy development and management. Dr. Nurwati is a member of IAENG and IEEE. She can be contacted at email: trinurti@ub.ac.id.

Eduard Muljadi received the Ph.D. degree in electrical engineering from the University of Wisconsin, Madison, US. From 1988 to 1992, he taught at California State University, Fresno. His current research interests include the fields of electric machines, power electronics, and power systems in general, with emphasis on renewable energy applications. Dr. Muljadi is a member of Eta Kappa Nu and Sigma Xi. He is involved in the activities of the IEEE Industry Application Society (IAS) and Power Engineering Society (PES). He is currently a member of the Industrial Drives Committee, Electric Machines Committee, and Industrial Power Converter Committee of the IAS, and a member of the Working Group on Renewable Technologies and the Dynamic Performance of Wind Task Force of the PES. He holds two patents in renewable energy conversion. He can be contacted at email: mze0018@auburn.edu.

Hazlie Mokhlis received a Bachelor of Engineering (B.Eng. (Hons)) degree and a Master of Engineering Science (M. Eng.Sc) in electrical engineering from the Universiti Malaya in 1999 and 2003, respectively. He received Ph.D. degree from the University of Manchester in 2009. He is currently a professor at the Department of Electrical Engineering, University of Malaya. Dr. Hazlie is actively involved in research as a principal investigator with a total amount of research grants of more than RM 3 million. He is the author and co-author of more than 300 publications in international journals and proceedings in the area of power systems and energy. Up to now, he had successfully supervised 40 Ph.D., 12 master's (by research), and 56 master's (mix-mode and course work) candidates. He is also active as a reviewer for many reputable journals and several international conferences in the area of power and energy systems. His outstanding research had been recognized by Stanford University in 2021, 2022, and 2023 as the Top 2% of scientists in the world. He can be contacted at email: hazli@um.edu.my.